



Variability in the coupling between sea surface temperature and wind stress in the global coastal ocean



Yuntao Wang¹, Renato M. Castelao^{*}

Department of Marine Sciences, University of Georgia, Marine Sciences Building, Athens, GA 30602, United States

ARTICLE INFO

Article history:

Received 16 December 2015
Received in revised form
31 May 2016
Accepted 16 July 2016
Available online 18 July 2016

Keywords:

Air-sea interaction
Coupling coefficient
SST
SST gradient
Fronts
Wind stress

ABSTRACT

Mesoscale ocean-atmosphere interaction between sea surface temperature (SST) and wind stress throughout the global coastal ocean was investigated using 7 years of satellite observations. Coupling coefficients between crosswind SST gradients and wind stress curl and between downwind SST gradients and wind stress divergence were used to quantify spatial and temporal variability in the strength of the interaction. The use of a consistent data set and standardized methods allow for direct comparisons between coupling coefficients in the different coastal regions. The analysis reveals that strong coupling is observed in many mid-latitude regions throughout the world, especially in regions with strong fronts like Eastern and Western Boundary Currents. Most upwelling regions in Eastern Boundary Currents are characterized by strong seasonal variability in the strength of the coupling, which generally peaks during summer in mid latitudes and during winter at low latitudes. Seasonal variability in coastal regions along Western Boundary Currents is comparatively smaller. Intraseasonal variability is especially important in regions of strong eddy activity (e.g., Western Boundary Currents), being particularly relevant for the coupling between crosswind SST gradients and wind stress curl. Results from the analysis can be used to guide modeling studies, since it allows for the *a priori* identification of regions in which regional models need to properly represent the ocean-atmosphere interaction to accurately represent local variability.

© 2016 Elsevier Ltd. All rights reserved.

1. Introduction

Satellite observations have revealed that sea surface temperature (SST) can have a profound influence on wind stress variability throughout the world ocean wherever there are strong SST fronts (Chelton et al., 2004; Xie, 2004). As summarized by Chelton and Xie (2010), surface wind increases over warm water in association with decreased stability through enhanced vertical mixing that deepens the atmospheric boundary layer and draws momentum from the upper boundary layer down to the sea surface. Over cold water, by contrast, surface wind decreases in association with increased stability that decouples the surface winds from the stronger winds aloft. When winds blow along a SST front, higher winds over the warm side of the front and weaker winds over the cold side of the front generate wind stress curl. If the winds blow across a SST front, wind stress divergence is generated. The wind stress curl and divergence anomalies vary linearly with the crosswind and downwind components of the SST gradient, respectively (Chelton et al., 2001). This coupling between SST and

winds has been widely observed, both in the open ocean (e.g., O'Neill et al., 2003, 2005, 2010; Chelton et al., 2004) and in coastal regions (e.g., Chelton et al., 2007; Castelao, 2012; Desbiolles et al., 2014). Since wind stress curl anomalies drive Ekman pumping (e.g., Pickett and Paduan, 2003), they can be associated with significant upwelling or downwelling, with important implications for the marine ecosystem. They can also lead to modifications in the SST distribution itself (O'Neill et al., 2003).

The influence of SST on wind stress is clearer in regions with strong SST gradients (Haack et al., 2008). The interaction between SST and wind stress is often quantified by coupling coefficients, defined as the slope of the regression between crosswind SST gradients and wind stress curl and between downwind SST gradients and wind stress divergence (e.g., O'Neill et al., 2010). Spall (2007) noticed that the coupling coefficient between wind stress and SST gradients has a significant quadratic dependence on the large-scale geostrophic wind speed. Large seasonal variability in front activity (e.g., Castelao and Wang, 2014) can lead to seasonal variations in the strength of the ocean-atmosphere interaction (Chelton et al., 2007). There is a general tendency for larger regression coefficients between downwind SST gradients and wind stress divergence compared to the coefficients between crosswind SST gradients and wind stress curl (Chelton et al., 2001; O'Neill et al., 2003; Seo et al., 2007). This is likely due to SST-induced wind

^{*} Corresponding author.

E-mail address: castelao@uga.edu (R.M. Castelao).

¹ Now at National Marine Fishery Service, NOAA.

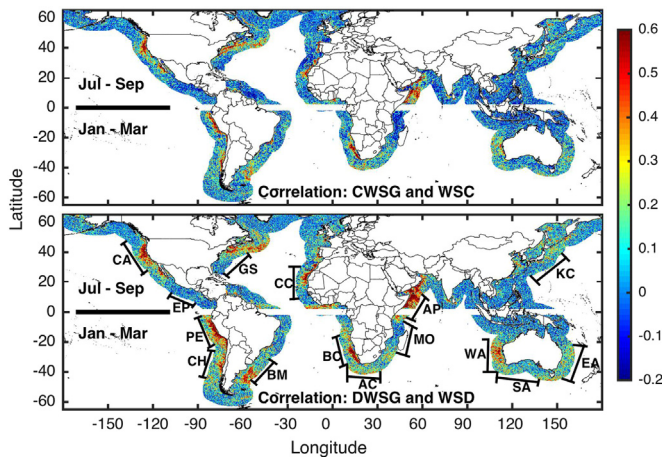


Fig. 1. Global maps of correlation between (top) crosswind SST gradient (CWSG) and wind stress curl (WSC) and between (bottom) downwind SST gradient (DWSG) and wind stress divergence (WSD). Only observations during summer (July to September in northern hemisphere, January to March in the southern hemisphere) were used for computing the correlations. CA: California Current System; EP: Eastern Tropical Pacific; PE: Humboldt Current off Peru; CH: Humboldt Current off Chile; BM: Brazil-Malvinas Confluence Zone; GS: Gulf Stream; CC: Canary Current; BC: Benguela Current; AC: Agulhas Current; MO: Mozambique Channel; AP: Arabian Peninsula; WA/SA/EA: Western/Southern/Eastern Australia; KC: Kuroshio Current.

direction gradient perturbations that enhance the divergence and reduce the curl response (O'Neill et al., 2010).

Despite the large number of studies investigating the coupling between SST and winds in the ocean, a systematic characterization of spatial and temporal variability in the strength of the coupling in coastal regions has not yet been done on a global scale. Studies have revealed large differences in the intensity of the coupling between different coastal regions (Chelton et al., 2007; Haack et al., 2008; Castelao, 2012; Desbiolles et al., 2014). However, it is not clear how much of these differences are due to actual variability in the strength of the coupling, and how much is due to methodological differences between the studies. Using multiple SST products, for example, with different resolutions and varying degrees of smoothing will result in different coupling coefficients (Castelao, 2012). Here, we use consistent satellite observations spanning seven years and standardized methods to investigate the ocean-atmosphere interaction in the coastal ocean on a global scale (Fig. 1). Coefficients are computed on a monthly basis, and subsequently used to quantify spatial and temporal variability in the strength of the coupling.

2. Methods

Wind data were collected by the SeaWinds scatterometer on board the Quick Scatterometer (QuikSCAT) satellite. A detailed description of the measurements is given by Chelton and Freilich (2005). The QuikSCAT spatial resolution is roughly 25 km, and measurements within 30 km from the coast are contaminated by radar backscatter from land in the antenna side lobes. Observations are available from July 1999 to Nov 2009. Sea surface temperature (SST) data were obtained by the Moderate-resolution Imaging Spectroradiometer (MODIS). Daily observations are available at approximately 5-km resolution since August 2002. Measurements within 5 km from land or from pixels flagged as clouds were discarded to avoid contamination. Regions farther than 800 km from the coast are discarded in this study in order to focus on coastal phenomena. The width of 800 km was chosen to guarantee that most fronts in the coastal ocean would be captured

by the analysis. In Eastern Boundary Current Systems, for example, the band of high frontal activity under the influence of upwelled water can extend for many hundreds of kilometers from the coast (van Foreest et al., 1984; Castelao et al., 2006; Wang et al., 2015) into the Coastal Transition Zone (Brink and Cowles, 1991), in some instances extending for as much as 1300 km offshore (Lutjeharms et al., 1991).

Here, we focus on the period from Nov 5, 2002 to Nov 4, 2009, when both observations of wind and SST are available simultaneously. All observations were time-averaged as in Chelton et al. (2007). Specifically, SST measurements were first averaged in overlapping 3-day periods at daily intervals. The crosswind and downwind components of the SST gradient was computed within each QuikSCAT measurement from the instantaneous wind stress field and the 3-day-averaged SST field centered on the date of the QuikSCAT observations. Crosswind SST gradients, for example, are defined as the cross product $\nabla \text{SST} \times \hat{\tau}$, where $\nabla = i\partial/\partial x + j\partial/\partial y$ is the two-dimensional gradient operator in Cartesian coordinates with unit vectors i and j in the zonal and meridional directions, respectively and $\hat{\tau}$ is a unit vector in the direction of the wind stress. SST, crosswind and downwind SST gradients, wind stress, wind stress curl and divergence were then averaged in 29-day periods at 7-day intervals. Anomalies for each variable were calculated as the deviation of each 29-day average from the respective seasonal average following Chelton et al. (2007). All observations were averaged onto a 0.25° latitude by 0.25° longitude grid.

Coastal regions along the entire globe were divided into 192 regions, with each region spanning approximately 500 km in the alongshore direction. Regions to the north of 65°N and to the south of 65°S were not considered. For each region, the 29-day averages at 7-day intervals were used to compute the coupling coefficients for each calendar month. The coupling coefficients are the slopes of the linear regressions between crosswind SST gradients (CWSG) and wind stress curl (WSC) and between downwind SST gradients (DWSG) and wind stress divergence (WSD) (Fig. 2). Chelton et al. (2007) showed that, for averaging periods longer than 11 days, the maximum correlations in the California Current System occur with a zero lag. As such, we followed their approach and did not apply any lag between SST gradients and wind variables. The linear regression analyses resulted in time series of coupling coefficients for each region spanning 84 months (7 years). Those time series were then used to calculate the corresponding mean and seasonal cycles. In order to quantify interannual, seasonal and intraseasonal variability, the monthly time series were first low-pass filtered using a 12 month filter (cosine-Lanczos filter; Mooers et al., 1968) to capture mostly interannual variability (Fig. 3), following Legaard and Thomas (2006). The differences between the original and the low-pass filtered time series correspond mostly to variability at seasonal or higher frequencies. We further applied a 6-month low-pass filter to the difference time series to isolate the seasonal signal. The residue time series after the removal of interannual and seasonal signals capture mostly intraseasonal variability (Fig. 3). For each region, the total variance of the time series of the coupling coefficients was approximated as the sum of the variance of the time series of interannual, seasonal and intraseasonal variability (Legaard and Thomas, 2007). The error due to the assumption (i.e., the difference between the sum of the variances of the time series for the three frequency bands and the variance of the original time series) is generally less than 14%.

Download English Version:

<https://daneshyari.com/en/article/4531578>

Download Persian Version:

<https://daneshyari.com/article/4531578>

[Daneshyari.com](https://daneshyari.com)